The IST Programme
Project No. 10378

SimBio

SimBio - A Generic Environment for Bio-numerical Simulation

http://www.simbio.de

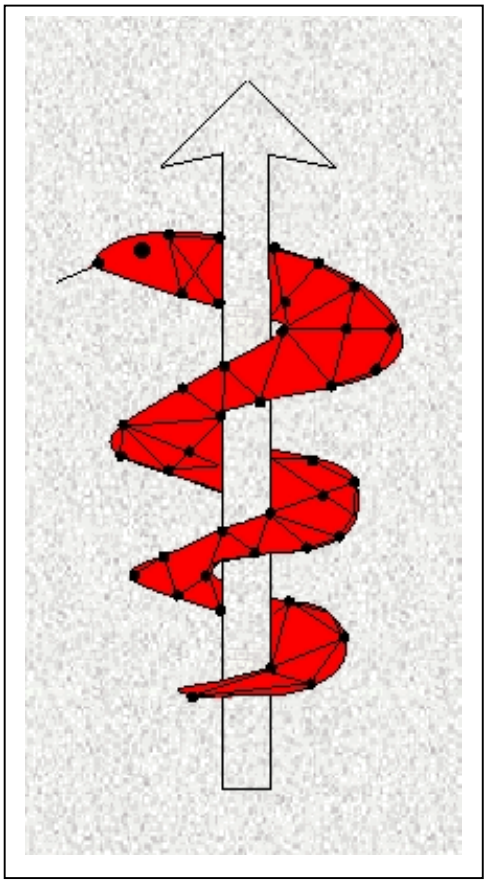

Final Evaluation Report 7.3

Status:	Final
Version:	1.0
Security:	Public
Responsible:	USFD
Authoring Partners:	{ESI, S&N}

Release History

Version	Date
1.0	29/06/03

The SimBio Consortium :
NEC Europe Ltd. – UK
A.N.T. Software – The Netherlands
Smith & Nephew - UK
CNRS-DR18 – France
University of Sheffield – UK
MPI of Cognitive Neuroscience – Germany
Biomagnetisches Zentrum Jena – Germany
ESI Group – France

1 Introduction 3
1.1 Purpose of Subtask 7.3 3
1.2 Review of Progress up to D7.3b. 3
2 Summary of ST7.3 Achievements 3
3 Software and hardware requirements 5
3.1 Image Processing Software 5
3.2 Simulation Software 5
3.3 Simulation Hardware 5
4 Modifications to the Template Mesh 6
4.1 Developing variable cartilage thickness meshes 7
5 Patient Data Acquisition 8
5.1 Clinical Measurements 11
5.2 Magnetic Resonance Scanning 11
5.3 Cine MR sequence 11
5.3.1 Limitations of the protocol 12
5.4 Static MR scanning Sequence 12
5.4.1 High resolution volume sequence 12
5.4.2 Motion Artefact 12
6 Image Processing and Patient Mesh Generation 13
6.1 Morphing the Template Mesh to Generate a Patient-Specific Mesh 13
6.1.1 Generating the Patient-Specific Binary volumes 13
6.1.2 Registering the Patient MR Volume to the Template MR volume 13
6.1.3 Examples of the automatic segmentation of patient images 14
6.2 Developing the Validation Method for the Knee Kinematics 17
6.2.1 Overview 17
6.2.2 Segmenting the Cine MR images 17
6.2.3 NAS Maribor IST tool 17
6.2.4 Segmentation Sensitivity Analysis for Cine Images 17
6.2.5 Repeatability Study 18
6.2.6 Registering the Cine MR Images to the Static volumes 19
6.2.7 Calculating the Euler angles and translations 19
7 Simulations 20
7.1 Mesh Template simulations 20
7.1.1 Simulation Issues 20
7.1.1.1 Penetration / Perforation Issues 20
7.1.1.2 Hour-glassing 20
7.1.1.3 Small volume elements 20
7.1.2 Exercise rig simulations 20
7.2 Patient-specific Simulations 21
7.3 Validating the simulations 24
7.3.1 Calculating the Euler angles and translations from the PAM simulation 24
8 Conclusions 28
9 Appendix A: Dynamic Registration Process: USFD 29

1 Introduction

1.1 Purpose of Subtask 7.3

As described in the Design Report (7.3a), the central objective of Workpackage 7 is to evaluate and validate the SimBio environment. It consists of three subtasks that will assess the utility of SimBio simulations for three medical applications, namely, Electromagnetic Source Localisation in the Brain, Bio-mechanical Head Modelling and Knee Loading Models with Prosthesis Design Problems.

This document is the final deliverable (c) of Subtask 7.3. It provides the final evaluation results for the third test application in the validation and evaluation of the SimBio environment with respect to the knee joint. The purpose of Deliverable 7.3c is to describe and discuss the overall evaluation of the Simbio Environment with respect to knee modelling and kinematic simulation and to indicate areas for post-project development.

1.2 Review of Progress up to D7.3b.

At the time of D7.3b being released, a template mesh of one knee joint had been generated and some simple rotation simulations had been completed. The initial results indicated that further refinement of the cartilage thickness of the template mesh was required to minimise contact problems between the cartilages and the menisci. In addition, knee flexion simulations driven by the loading from the exercise rig needed to be carried out for the template mesh and for selected pre and post-operative patient meshes.

Testing of the automated segmentation and meshing tools (Vsegment3d and Vgrid, respectively) that work well for brain tissue were found to be less than optimal when applied to the knee joint. It was planned to investigate a new approach proposed for segmentation and meshing that would combine the two processes, the "mesh template" approach. A detailed discussion of this method and the algorithms developed to achieve it can be found in D1.1c (p7-9). This deliverable will focus on the application of the mesh morphing method to generating patient–specific meshes and the results of simulations conducted using the morphed meshes.

2 Summary of ST7.3 Achievements

Subtask 7.3 focussed on the application of SimBio tools to the study of the human knee. Three subtasks were identified, covering simulation, validation and evaluation. The primary achievements have been:

- The selection of appropriate high-resolution static and fast-acquisition psuedo-dynamic mri scan sequences for segmentation of bone, articular cartilage and meniscus and for kinematics evaluation respectively. Details are presented in the public deliverables.
- The development of an MRI-compliant exercise rig for kinematic evaluation under relatively controlled conditions.
- The establishment of a dataset of three-dimensional medical images of the knees of a series of normal subjects and of patients pre- and post-operation, containing both high resolution static scans and pseudo-dynamic scans. Eleven patients were recruited. All were MR scanned pre-operatively, while four were not recalled for post-operative scanning due to additional pathologies or the necessity to implant metalwork into the knee during the operation. Five patients had data that were suitable for simulation trials. The pathologies included three medial meniscal injuries, one lateral meniscal injury and a postero-lateral corner injury.
- The development of a new tool, exploiting the registration algorithms developed in workpackage one, for quantification of knee kinematics from the dynamic scan data. We believe that these tools offer an accuracy in the assessment of knee kinematics that was hitherto unachievable.

- The investigation of the application of a range of segmentation and mesh generation algorithms to the construction of patient-specific knee meshes. We believe that we have demonstrated that the best approach for knee applications is the morphing of a template mesh. Mesh smoothness is an important issue for the evaluation of joint kinematics.
- Contribution to the development of the novel SimBio template-based patient-specific mesh generation algorithm (see Workpackage One), and its testing on the SimBio dataset.
- Construction of a template finite element knee model of the reference dataset. The final template mesh consisted of 3,464 8-node solid elements, 13,120 shell elements, the majority of which were defined within rigid bodies representing the bone components of the knee and the remainder used in the contact interface definition), and 232 bar/beam elements.
- The simulation of the kinematics of the knees of the study group (normal and patient applications), and comparison with the results of the supporting experimental programme.

There has been some change of emphasis as the programme has progressed:

- The construction of patient-specific meshes for the knee proved more difficult than was originally anticipated, primarily because the intensity-based segmentation algorithms did not produce good results in the context of the knee. This increased the amount of effort that went into the patient-specific mesh generation within Subtask 7.3.
- The development of a specification for a meniscal prosthesis was not undertaken, partly because Smith and Nephew, the commercial partner for the knee tasks, had reduced interest and partly because effort was directed elsewhere.
- Significant effort was expended in the support of the new workpackage, 7.4. This was regarded as a very positive aspect of the programme, because a number of issues relating to the dissemination of the SimBio tools to potential customer sites (which otherwise would not have been addressed within the work programme) were resolved.

A protocol adopted for patient studies might follow that adopted within this workpackage.

- The patients were scanned in Sheffield, (the data being anonymised at acquisition); the DICOM data for each patient was transferred through the Hospital firewall to a secure University SGI machine where it was converted to the VISTA file format using the WP1 image processing tools. The patient VISTA image volume was then transferred to the Linux SCore Cluster at NEC in Bonn where it was registered to the pre-segmented template volume using the *vreglocal3d* algorithm. The registration process takes approximately 40 minutes per patient using a single processor (there is no parallel version available at present). Ideally the image processing should take place locally but for demonstration purposes this has been done using the remote NEC computing facilities. In comparison, using a local 2.4GHz Linux P4 (Intel compiler), the registration process takes approximately 20 minutes, hence the reason for not parallelising the registration algorithm. Once the registration is complete, the mapping produced is applied to the template mesh, using the *vtransform* algorithm to morph the template mesh into a patient-specific mesh, which takes less than a minute.
- Once the mesh had been morphed it was transferred back to Sheffield, where patient-specific information, (e.g. femur lengths, limb masses, applied forces) were applied to the PAM "include" file, (a specification file of all boundary conditions) to prepare the simulation run. The new VISTA mesh was imported into PAM GENERIS, associated with its include file and saved as a PAM-specific .pc file. This .pc file was transferred back to the NEC SCore Cluster and run on the PAM-SAFE parallel solver. A simulation run takes approximately 7.86 hours to reach approximately 45° of knee flexion (300ms) using 4 processors. In contrast, using three processors on the Origin 2000 SGI (four 250MHz R10K processors, 2560Mb RAM) at USFD the same run takes 25.8 hours.

Based on the experience and expertise developed within SimBio, we would suggest that:

- The mesh morphing method has been demonstrated to work well for generating patient-specific finite element knee meshes. Despite the amount of time spent developing the template mesh, we believe that the template mesh approach is the most appropriate one for the knee, because of the problems demonstrated in segmenting clinical knee images by an

intensity-based approach and the difficulties in obtaining a mesh that is sufficiently smooth for kinematic simulations.

- Further development will be required to take into account major pathologies, such as significant meniscal tears, by generating template pathologies from which a clinician could select the most appropriate prior to morphing the template mesh. At present, the algorithm will attempt to "crush" elements in the template to best match the losses of tissue indicated from the patient image. There are several ways in which this issue could be addressed, but an examination of the vector fields produced by the registration process and the implementation of a decision tree based on their properties has great potential.
- The kinematic results from the simulations do not demonstrate clearly the clinically important internal "screw-home" rotation of the femur on the tibia from partial flexion to full extension, which is seen clearly in the validation trials. It is likely that additional work will be required to model the complex nature of the cruciate and collateral ligaments. At the start of the programme we felt that available 3-D material models and finite elements were not developed sufficiently to address this. Current advances may permit solid modelling of the ligaments to be investigated as a post-project development. The development of a more advanced template featuring these elements is recommended.
- Further work is required on the measurement of muscle forces and of the pretension in ligaments in order to improve the applicability of the simulations to the *in vivo* condition.

3 Software and hardware requirements

3.1 Image Processing Software and Platforms

The tools to undertake the image registration and mesh morphing using the mesh template method were developed at USFD using C++ and have been compiled for and tested on a high specification PC (2.4 MHz P4, running Linux (RedHat v7.2), a SGI Origin 2000 (four 250 MHz R10K processors, 2560 Mb RAM, IRIX 6.5) and the Linux-Score PC cluster at NEC (64 nodes). In addition, the executables have also been tested on a Win 2000 PC by utilising the freeware "Cygwin" DLL (http://www.cygwin.com/) to emulate the Linux environment. The image processing and mesh generation software tools released by Workpackage 1 make use of the Vista file format.

3.2 Simulation Software

As stated in the Design Report, the PAM-SUITE™ software provided by ESI, (Paris) was utilised to undertake the simulations. The suite consists of PAM-GENERIS™, a pre-processor that permits an existing mesh to be prepared for use with either the 2 explicit finite element solvers, PAM-CRASH™ or PAM-SAFE™, and the PAM-VIEW™, the suite's post-processor. For the purposes of the SimBio project, the PAM-SAFE™ solver was used, which was most appropriate for the simulations that were planned. ESI, (Rungis, France) modified their pre-processor, PAM-GENERIS™ to be able to import and export Vista format meshes. This was a necessary step because the template mesh had been completed in PAM-GENERIS and needed to be exported in a format that could be morphed using the WP1 tools.

3.3 Simulation Hardware

A SGI Origin 2000 (four 250 MHz R10K processors, 2560 Mb RAM, IRIX 6.5) was used for the mesh template simulations conducted at USFD, while the patient simulations were undertaken using remote computing at NEC on the Linux-Score PC cluster (64 nodes).

4 Modifications to the Template Mesh

Two significant changes to the template mesh were made. The first was provoked by an injury (unrelated to Simbio) to the volunteer (A) used to develop the mesh which was thought would preclude the additional cine MRI imaging necessary to validate the knee motion (as stated in p8 of D9g). Therefore, a new volunteer (B) was scanned and a new template mesh developed. The development of the new surface mesh used for the rigid bodies made use of automated image processing tools developed at USFD to surface contour between the segments of the MR slices. After extensive testing of this mesh, the simulation results indicated that (similar to the issue with Vgrid generated meshes), the resultant mesh was insufficiently smooth for the sliding contact problems required for the knee (Figure 1 and Figure 3).

The second modification to the template mesh involved utilising the inherently smooth mesh developed from volunteer A and using it to develop a smooth mesh of volunteer B. The MR images from (A) were registered to the MR images from (B) using the WP1 registration tools. The mapping function generated from the registration permitted morphing the smooth template mesh A to form a new smooth template mesh for volunteer (B) (Figure 2 and Figure 4).

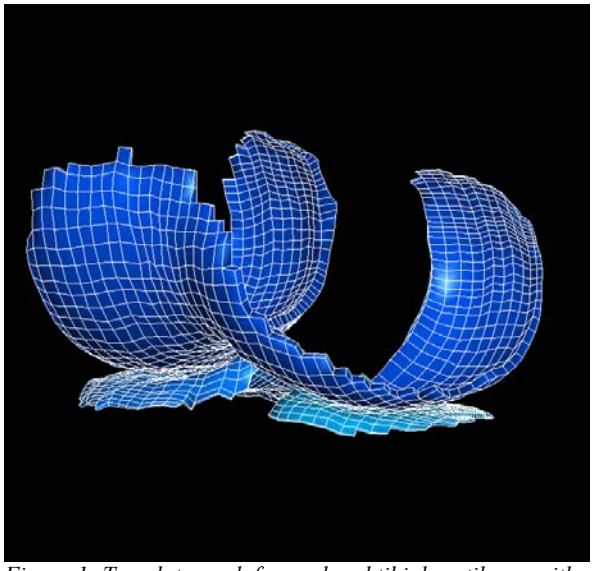

Figure 1: Template mesh femoral and tibial cartilages with insufficiently smooth surfaces

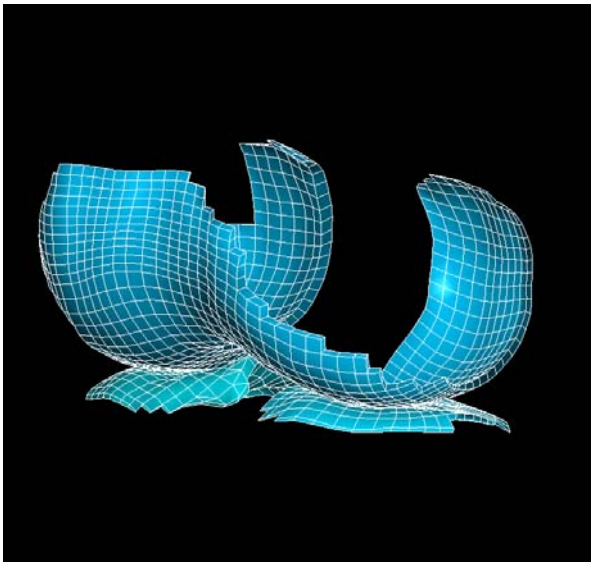

Figure 2: Template mesh femoral and tibial cartilages with smooth surfaces

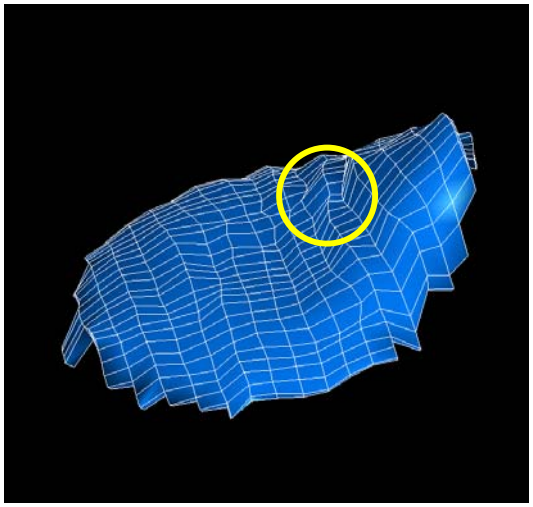

Figure 3: Insufficiently smooth lateral cartilage of template mesh

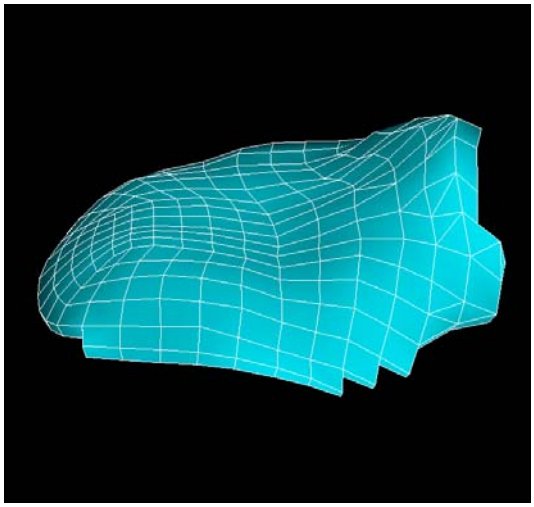

Figure 4: Smooth lateral cartilage of template mesh

4.1 Developing variable cartilage thickness meshes

As discussed in D7.3b p12, the first version of the template mesh (volunteer A) utilised constant thickness cartilages generated by extruding a surface normal 2mm from surface elements identified in the cartilage regions. This process was carried out because the initial MR sequence had insufficient resolution to segment the cartilages manually. The process of creating the second smooth mesh for volunteer B involved generating binary volumes for the femur and tibia from the volunteer A mesh model and mapping the femur and tibia segments from the volunteer B model to it. Essentially this process "stretched" the outer surface of the bone segments to map to the outer surface of the cartilages. The cartilage elements were then formed by connecting the original nodes on the bone surface to the new outer nodes on the mapped bones surface to generate 8-node hexahedral elements.

The final template mesh consisted of 3,464 8-node solid elements, 13,120 shell elements, the majority of which were included as part of a rigid body and the remainder used in the contact interface definition) and 232 bar/beam elements.

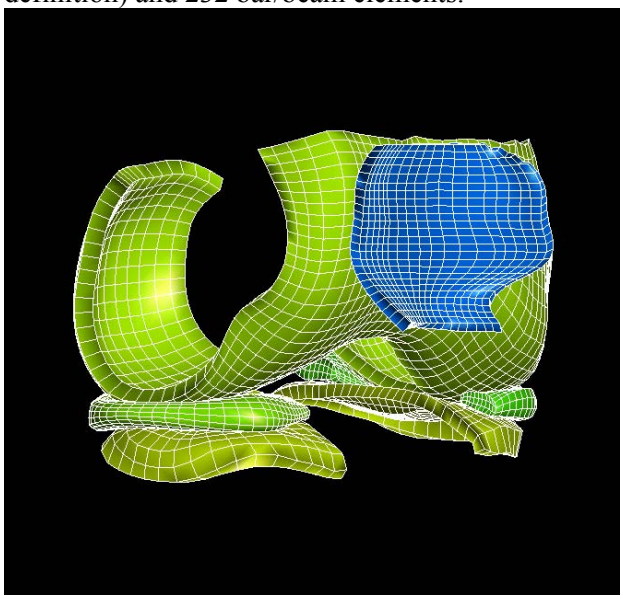

Figure 5: The smooth constant 2mm thickness cartilages from the original mesh template

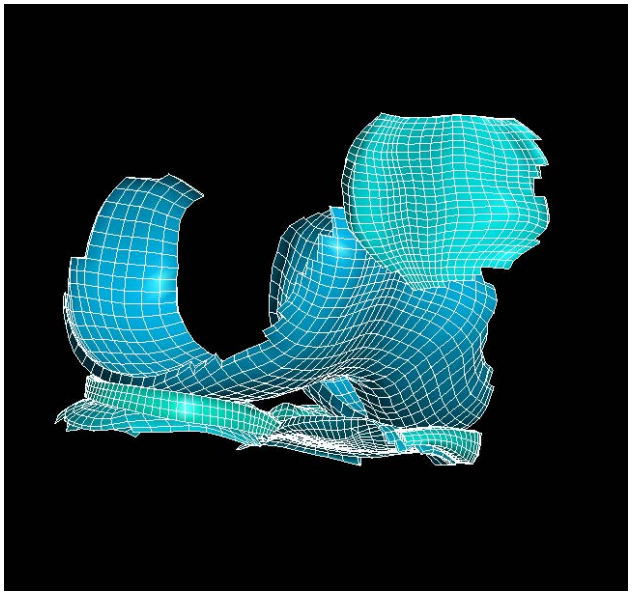

Figure 6: The resultant new template cartilages generated by morphing those in Figure 5

5 Patient Data Acquisition

All of the patients gave informed consent to participate in the study as approved by the Trent Ethics Committee and their details were anonymised. A total of eleven patients were recruited, but for various reasons (see Table 1) six patients or their datasets were not suitable for complete processing. Table 1 gives a detailed breakdown of the patients that were scanned, the scan data acquired, whether the data was suitable for dynamic motion validation, whether the data was suitable for a simulation trial and the clinical history of the patient.

As can be seen in Table 1, after the arthroscopic procedure, four patients were found to have pathologies additional to their initial diagnosis that made them unsuitable for a simulation trial or for repeat scanning. In the case of one patient, during the operative procedure it became necessary to implant titanium metalwork into the knee, which prevented repeat scanning (due to expected image artefacts and ethical restrictions). The static MR sequence for three patients early in the data collection process showed significant motion artefact for the static volumes, despite the extensive testing of the sequence on volunteers prior to patient data collection.

The four patient codes that were suitable for simulations were: MN02, MN03, (medial meniscal tears), MN08 (a lateral meniscal tear) and AC03 (a postero-lateral corner injury resulting in an unstable knee).

Patient Information

Patient Code	Pre-Op Number	Pre-Op Scan Date	Post-Op Number	Post-Op Scan Date	Motion Artefact Pre	Motion Artefact Post	Expected Pathology	Actual Pathology	Useable Kinematic Data	Useable for Simulation	Gender/Side/Age
MN01	64290	11/3/02	64291	02/5/02	YES	YES (small)	Medial meniscus	Medial meniscus	YES	NO	M/L/49
MN02	65334	07/5/02	65336	20/6/02	NO	NO	Medial meniscus	Medial meniscus	YES	YES – PRE / POST	M/L/33
MN03	65374	08/5/02	65375	07/8/02	NO	YES (v. small)	Medial meniscus	Medial meniscus	YES	YES - PRE	M/R/49
MN04	65376	15/5/02	65507	27/6/02	YES (v. small)	YES (small)	Lateral meniscus	Lateral meniscus + subchondral cyst	YES	Likely PRE	F/L/67
MN05	66474	08/7/02	No recall	-	YES (flexion)	-	Medial meniscus	OA knee	YES - Pre	NO	F/L/52
MN06	66568	15/7/02	No recall	-	YES (v. small)	-	Medial meniscus	Patello-femoral	YES - Pre	Likely PRE	F/L/42
MN07	67331	19/8/02	No recall	-	NO		Medial meniscus	Patello-femoral	YES – Pre T1/T2* (good flexion)	YES – PRE)	M/L/35
MN08	67759	12/9/02	68247	20/11/02	NO		Lateral meniscus	Large lateral tear	YES T1/T2*	YES - PRE	M/R/35
AC01	9482	13/2/02	63876	10/4/02	YES	NO (40 slices)	ACL repair	ACL	YES	POST	F/L/35
AC02	64509	04/4/02	No recall	-	YES	Not scanned (unsuitable due to metalwork)	ACL repair	ACL	YES - Pre	NO (Metal)	M/R/21
AC03	65675	23/5/02	65676	04/7/02	NO	Volume not scanned	Postero-lateral corner +?ACL	Postero-lateral corner	YES	YES	M/L/27

Table 1: Patient Magnetic Resonance Information sheet

5.1 Clinical Measurements

All the patients were operated on by the Consultant Knee Specialist (DRB) working at the Sheffield Centre for Sports Medicine. The recruitment of patients, acquisition of their informed consent to participate, collection of clinical measurements and supervision of the MR acquisition procedure was undertaken by the additional surgeon employed for one year to work on the Simbio Project. The measurements made were necessary to customise the simulations for suitable limb masses, lengths and inertias.

5.2 Magnetic Resonance Scanning

All of the patients were scanned using a standard 1.5T Eclipse closed bore MR scanner (Philips Medical Systems), either at the Royal Hallamshire Hospital or Northern General Hospital, which are both part of the Sheffield Teaching Hospitals Trust (STHT) in Sheffield. The MR data from the patients were anonymised at acquisition. Both MR acquisition sequences utilised the flexible general-purpose radio-frequency surface coil positioned around the knee joint as discussed in D7.3b (Section 2.2.1). The cine sequence was acquired first, with the patient positioned onto exercise rig by the surgeon and the radiographer. The patient was asked to undergo a series of practice knee flexion/extension motions prior to image acquisition, while the motion was viewed from the control room. Once the clinician was satisfied that the motion was repeatable and at even increments, the radiographer acquired a localiser image for each end of the range of motion to determine where the field of view should be defined. These images were taken to ensure that the knee remained within the specified field of view during the motion. The patient started the motion from fully extended, and moved to the each subsequent position under the verbal control of the radiographer in the control room.

Following the cine sequence, the patient was released from exercise rig and positioned for the high-resolution static sequence, which generally required 20 minutes of scanning time.

Once acquired, the DICOM data for each patient backed up onto optical disk (provided by STHT) and then transferred through the Hospital firewall to a secure University SGI machine.

5.3 Cine MR sequence

Two cine sequences were tested for the "dynamic" motion validation protocol. The first was a T2* gradient echo sequence that used a 256 x 256 acquisition matrix resulting in an in-plane pixel resolution of 1.63 x 1.63 mm as shown in Figure 7. For this protocol, 36 images were acquired, consisting of six sagittal slices through the knee at six different flexion angles in the exercise rig. The second and final sequence used for scanning the latter patients was a T1-weighted gradient echo cine sequence that used a 512 x 512 (interpolated) acquisition matrix resulting in pixel resolution of 0.82 x 0.82 mm. This sequence gave improved visualisation of the bone boundaries (as shown in Figure 8) with an added benefit of reduced scan times (1min 30s compared with 3 min 30s) and an additional image through the centre of the joint over the original T2* gradient echo sequence.

Table 2: Details of the 2 Cine MR imaging sequences

Sequence Type (Using GP flex coil)	Size	Number of slices	Slice thickness (mm)	Total scan time (s)
T2* CINE: TR=29ms, TE=13.0ms, Flip angle=20° Fixed data, even spacing using distortion correction algorithm Field of view: 41.8 x 41.8 cm effective pixel size = 1.63 mm	256 x 256	36 (6 slices per position for 6 knee flexion angles)	3	210

T1 CINE: TR=10ms, TE=2.0ms, Flip angle=90° Fixed data, even spacing using distortion correction algorithm Field of view: 41.9 x 41.9 cm effective pixel size = 0.82 mm	512 x 512	42 (7 slices per position for 6 knee flexion angles	3	90

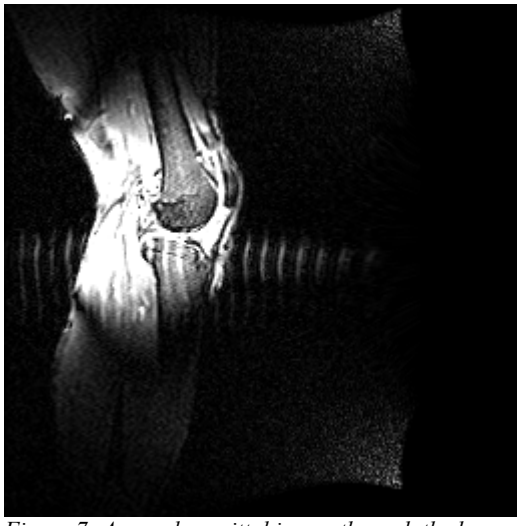

Figure 7: A sample sagittal image through the knee of MN07 using the original T2 dynamic sequence*

Figure 8: A sample sagittal image through the knee of MN07 using the modified T1 dynamic sequence (scaled by 50% for this image)

5.3.1 Limitations of the protocol

During the testing phase, it was found that moving too far from the isocentre of the MR field, (typical for knee flexion angles greater than 45°) resulted in significant distortions of the images. To minimise this effect and to ensure the best images possible, the distortion correction algorithm supplied with the Philips Eclipse software was utilised, together with a physical constraint to prevent the patient over-flexing.

The knee motion visualised in MR scanner is constrained compared to what might occur in real-world knee motion, such as walking, due to the constraint upon the ankle joint and restriction of the MR-bore. This was a necessary limitation to give more information about the boundary conditions in the finite element knee model by constraining the ankle in the rig to ensure that force application was derived from knee motion rather than plantar flexion of the ankle.

5.4 Static MR scanning Sequence

5.4.1 High resolution volume sequence

The final sequence used for patient image acquisition was a T2* gradient echo volume sequence (512 x 512, with an in-plane pixel resolution of 0.35mm).

5.4.2 Motion Artefact

Although the static sequence had been tested thoroughly with six volunteers and no problems encountered, the first patient volume acquired (MN01) showed motion artefact. Because the scan acquisition took approximately 20 minutes to complete, the scanner software enforced the scan to be acquired as two batches. Signal averaging takes place over the duration of a batch, so if two separate batches are collected for one acquisition then any movement made by the patient during a batch will be averaged and will appear as a discontinuity between the two batches.

A firm foam support was utilised under the knee to minimise motion artefact. Too stiff a material may have resulted in soft tissue deformation and too compliant would have resulted in sag of the support during the scan.

In an attempt to avoid motion artefact for one patient early in the study (AC01), a 40-image sequence was acquired. This was not in adherence to our specified protocol but was used as a means to guarantee a static dataset free from motion artefact. This did cause some additional work for the registration routine as will be discussed in Section 6.1.3.

6 Image Processing and Patient Mesh Generation

6.1 Morphing the Template Mesh to Generate a Patient-Specific Mesh

6.1.1 Generating the Patient-Specific Binary volumes

Once the patient DICOM data had been transferred to the secure University SGI Origin 2000, it was converted to the VISTA file format using the WP1 image processing tools. The patient VISTA image volume was then transferred to the Linux SCore Cluster at NEC in Bonn where it was registered to the pre-segmented template volume using the *vreglocal3d* algorithm. The registration process takes approximately 40 minutes per patient using a single processor (there is no parallel version available at present). Ideally the image processing should take place locally but for demonstration purposes this has been done using the remote NEC computing facilities. In comparison, using a local 2.4GHz Linux P4 (Intel compiler), the registration process takes approximately 20 minutes, hence the reason for not parallelising the registration algorithm. Once the registration is complete, the mapping produced is applied to the template mesh, using the *vtransform* algorithm to morph the template mesh into a patient-specific mesh, which takes less than a minute.

6.1.2 Registering the Patient MR Volume to the Template MR volume

For the areas of interest, particularly the articulating surfaces of the femoral and tibial condyles, the cartilages and the menisci, the automatic segmentation from the registration of the patient images to the template images is excellent and is comparable to the expected results from the an expert users. However, in areas of the images outside the region of interest, where the MR contrast is poor, the results are not so good. This type of artefact can be seen in the edge of the femoral condyle and superior aspect of the patella for the segments of patient MN08 (as highlighted in pink in Figure 12) and the patella of ACO3 (Figure 13).

6.1.3 Limitations of the protocol and refinements

In cases where the static UFSD MR protocol had not been adhered to limitations with the registration algorithm were noted. Typical examples were where only 40 MR images were acquired (as with patient AC01), which resulted in features in the image being too close to the edge of the image. The algorithm is sensitive to such close cropping. A small modification was made to the code to ensure that it coped with edge features more reliably.

In other cases, (as with some sequences acquired by SBM), where the flexion angle varied significantly from the 10° of flexion of the template image difficulties were found with achieving an acceptable segmentation. However, a satisfactory result could still be achieved following a modification to the code that permitted a user-specified region of interest to be applied.

6.1.4 Error propagation

In a set of template images where an error had been introduced into an area outside of the region of interest (on the femoral shaft), test segmentations to other sequences demonstrated that the error will propagate into the segments that are generated automatically. It is therefore important to ensure that the template is free from errors prior to generating new segments. This is particularly important where the segments are to be used to generate a mapping for creating a patient-specific mesh. In such cases, the error would propagate into the resultant mesh.

6.1.5 Examples of the automatic segmentation of patient images

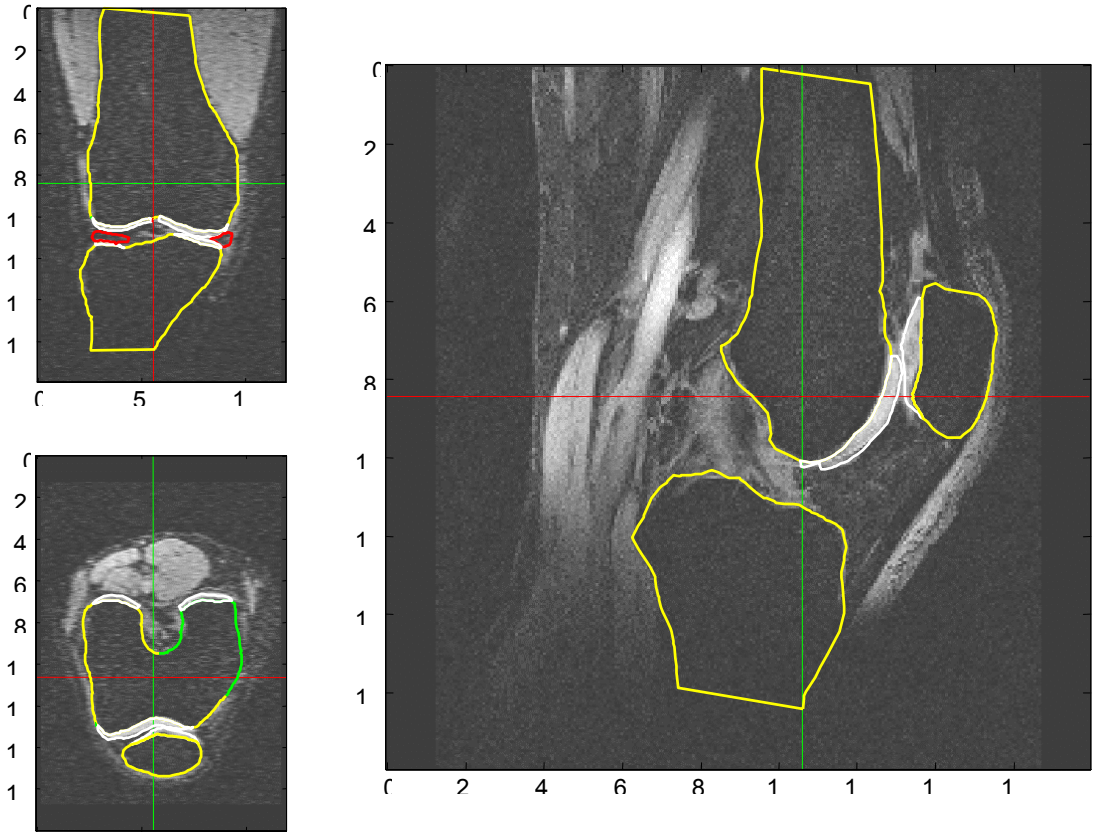

Figure 9: Sample segments for patient MN02

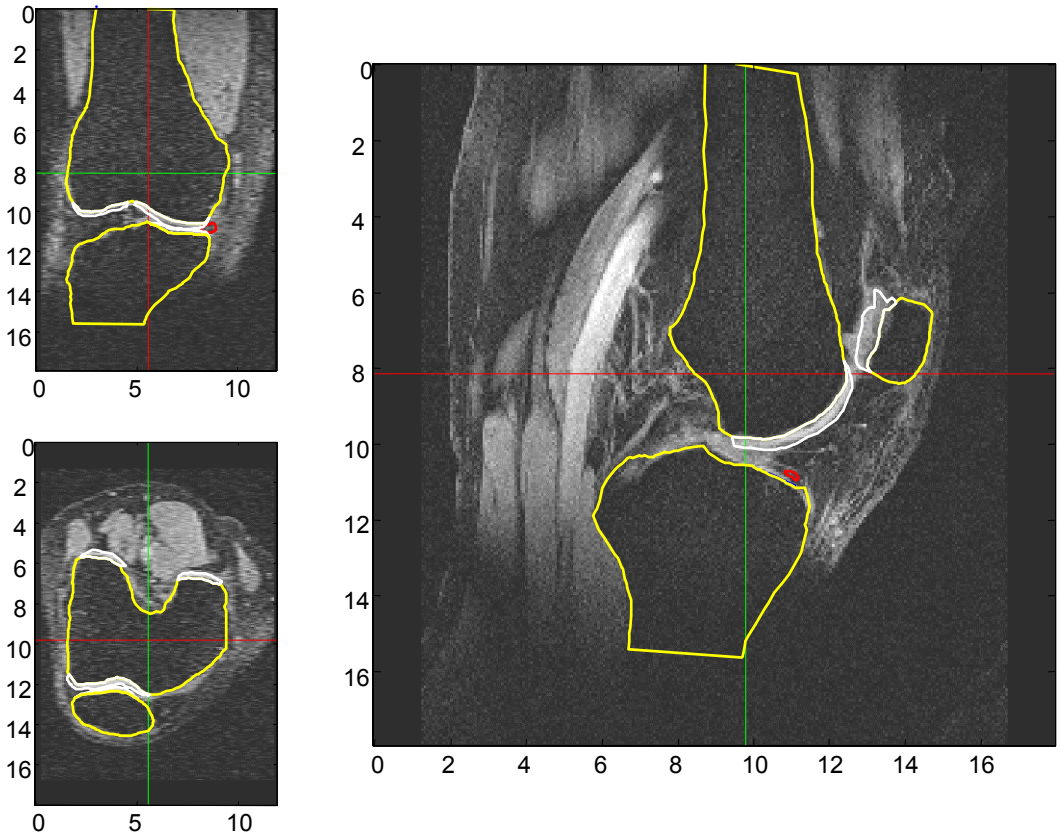

Figure 10:Segments for patient MN03

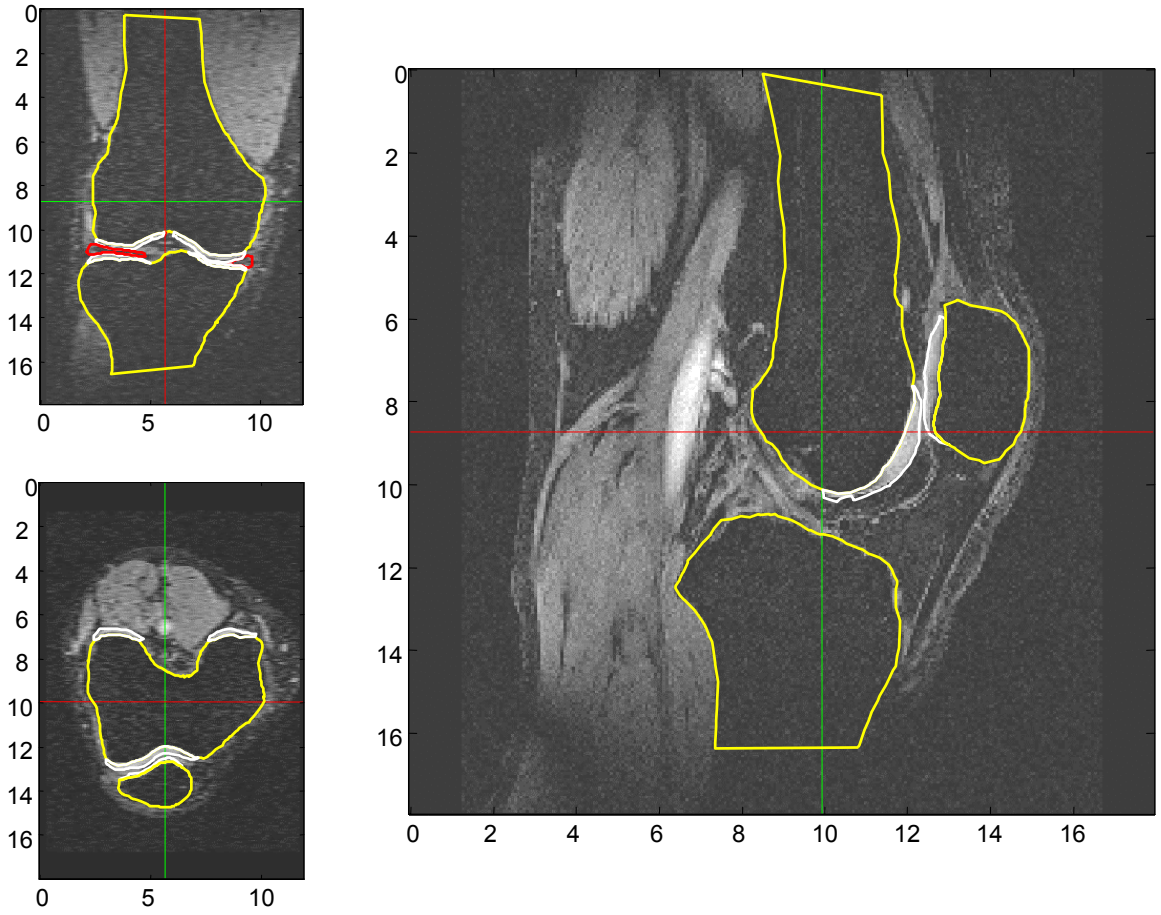

Figure 11: Sample segments for patient MN07

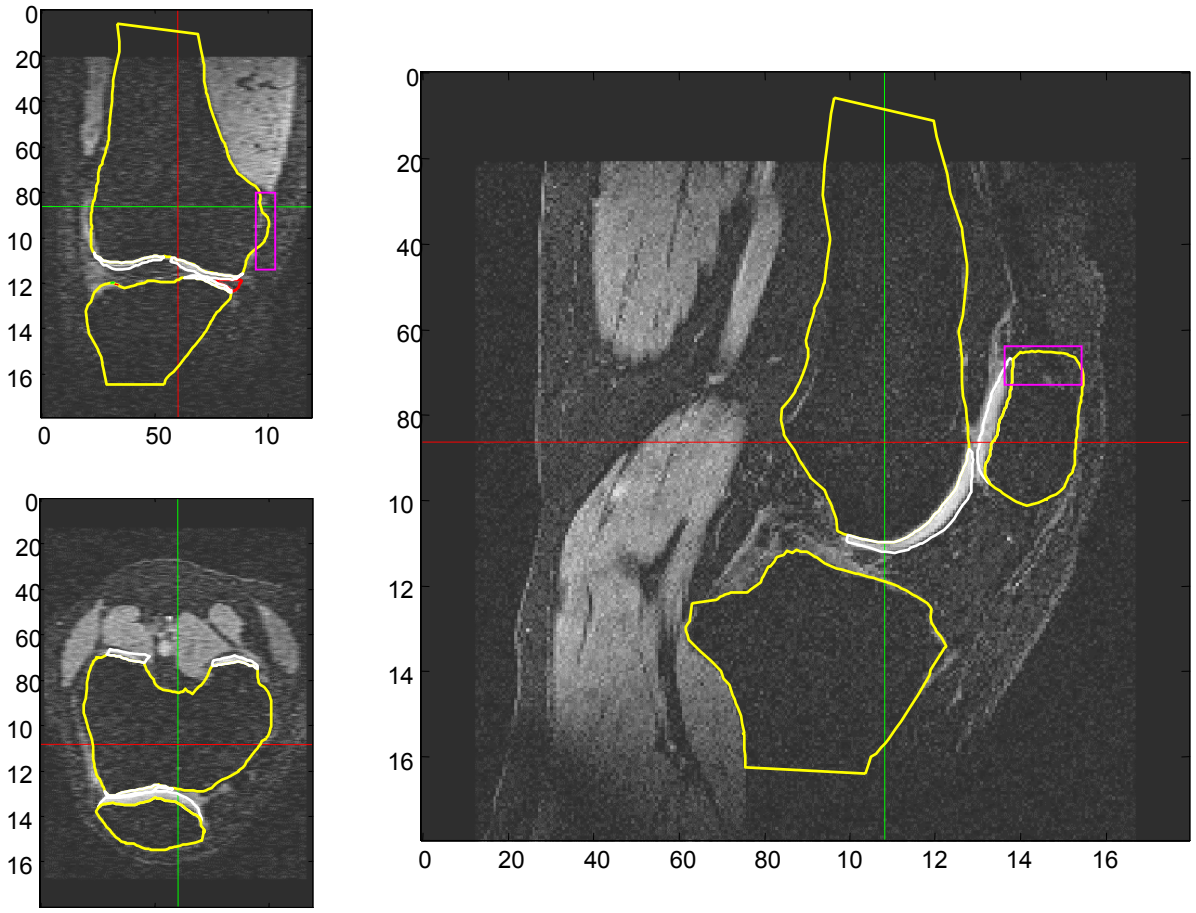

Figure 13: Sample segments for patient MN08

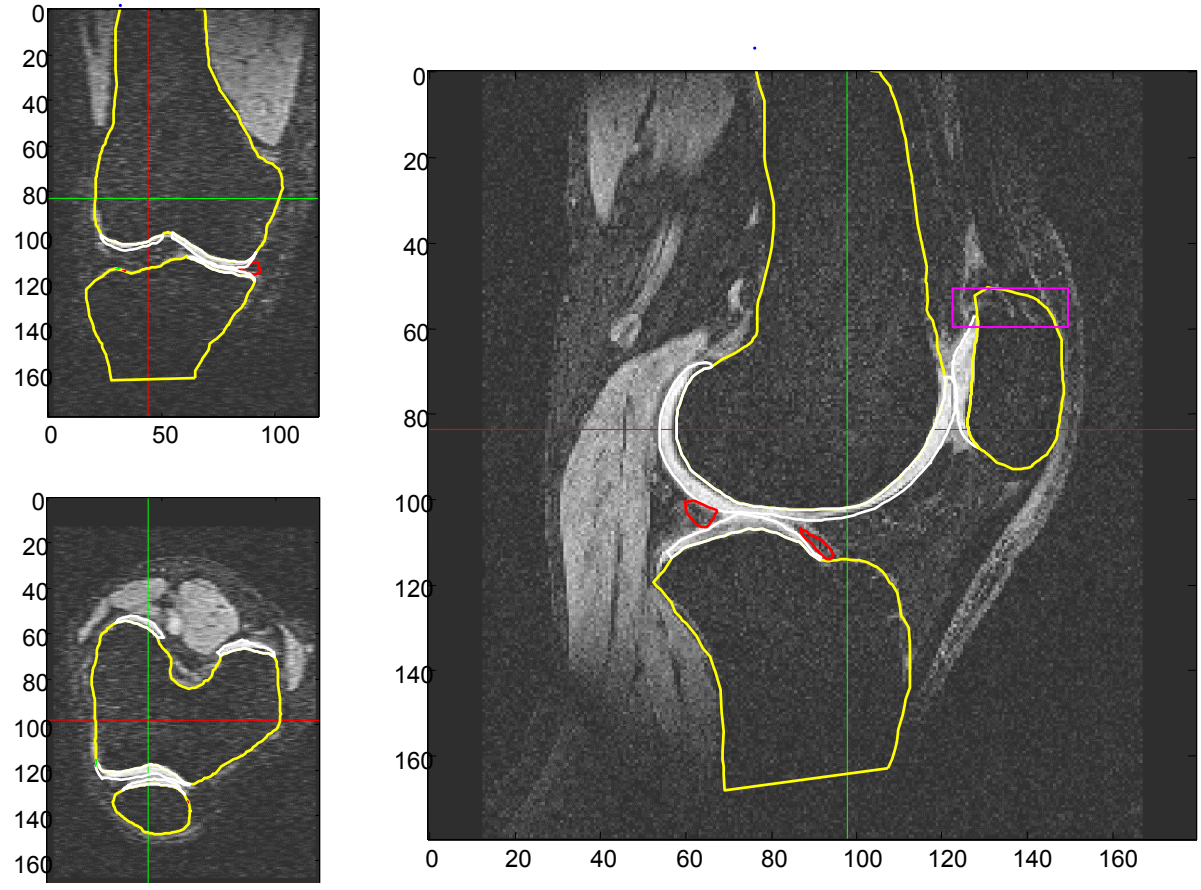

Figure 12: Sample segments for patient AC03

6.2 Developing the Validation Method for the Knee Kinematics

6.2.1 Overview

The procedures used for the dynamic registrations necessary for validating the motion in the PAM simulations are shown in Figure 14 below. All the code was developed in Matlab at USFD and was not intended for general release. The functions developed are shown in yellow. To permit the Simbio-NAS supplementary project to progress efficiently, the code was released to Maribor and a comprehensive help document supplied (as shown in Section 9).

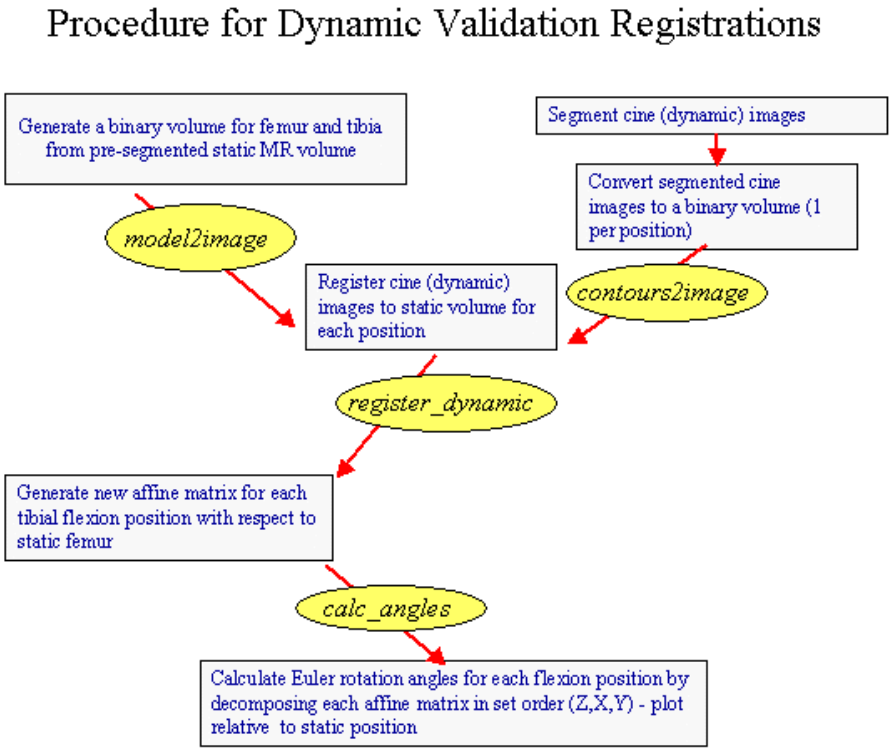

Figure 14: Flow chart indicating the dynamic registration procedure

6.2.2 Segmenting the Cine MR images

The surgeon employed to work on the Simbio Project segmented the femur and tibia from the sparse MR cine images manually using the commercial software SURFDriver™ 3.5. As described in D7.3b (p10), this software was also used to generate the initial segments for the template from the static MR images to aid the process of template image segmentation and mesh generation. The segmented images and template mesh were the intended deliverable and not the manual segmentation software.

6.2.3 NAS Maribor IST tool

The introduction of the NAS extension to the Simbio Project has resulted in the development of the IST (Image Segmentation Tool) software, which replaces the requirement for SURFdriver™.

6.2.4 Segmentation Sensitivity Analysis for Cine Images

As indicated in D7.3b, a key step in ST7.3 was the development of a non-invasive and accurate method to validate the motion of the FE knee mesh in the simulations. Because the method is being used a validation tool it is critical to demonstrate the sensitivity of the method to errors in segmentation.

Theoretical sensitivity analyses were performed by introducing typical errors (yellow contours) to the true segments (red images) for each level and type of noise. Two types of error were introduced, random, which are representative of intensity-based segmentation, and smooth, which are representative of manual segmentation. For each type of error, two error sizes were tested, 1 and 2. For random errors, '1' represents a 1-mm error, while '1' for smooth errors essentially represents a

smoothed 1-mm error. . Once the errors were introduced, the registrations of the binary volume for the femur and tibia to the manual segments to the femur and tibia were carried out 10 times for rotation angles up to 40 degrees about the primary flexion axis and up to 10 degrees for rotations about the secondary axes. The results were plotted as the calculated angle against the applied rotation angle. Only one axis rotation was applied at a time in all cases, thus there should only be 1 line on the graph that approximates 45° (i.e. for an applied rotation of 30 degrees about Z, ideally the returned angle should also be 30 degrees about Z). The error bars shown indicate 1 standard deviation over all registrations.

The results appear to be insensitive to segmentation errors of up to 30° in the primary flexion axis and indicate that for smooth errors of 2mm, the results deviate markedly from the expected angles for tibial flexion angles greater than 40°. However, the total knee flexion possible in the MR scanner is 40°, and only half of this (i.e.20°) would be expected to come from the tibia alone. Therefore, for the angles that are possible in the MR scanner when constrained by the exercise rig, the results appear not to be sensitive to the typical maximal errors that might occur during a manual segmentation.

The full results can be found in Appendix B.

6.2.5 Repeatability Study

To indicate whether the whole process was repeatable, three independent cine scans were acquired of Volunteer B, capturing three different knee motions spread over different days. These were segmented independently and processed through the validation method described in Section 6.2.2. The calculated rotation angles are shown in Figure 15. Although there is a noticeable difference in the magnitude of the external rotation of the femur in the first few degrees of knee flexion (probably indicative of a differing starting position), the direction is consistent. Once 15° of knee flexion had been reached, the knee appeared to be stable in internal/external rotation and varus/valgus.

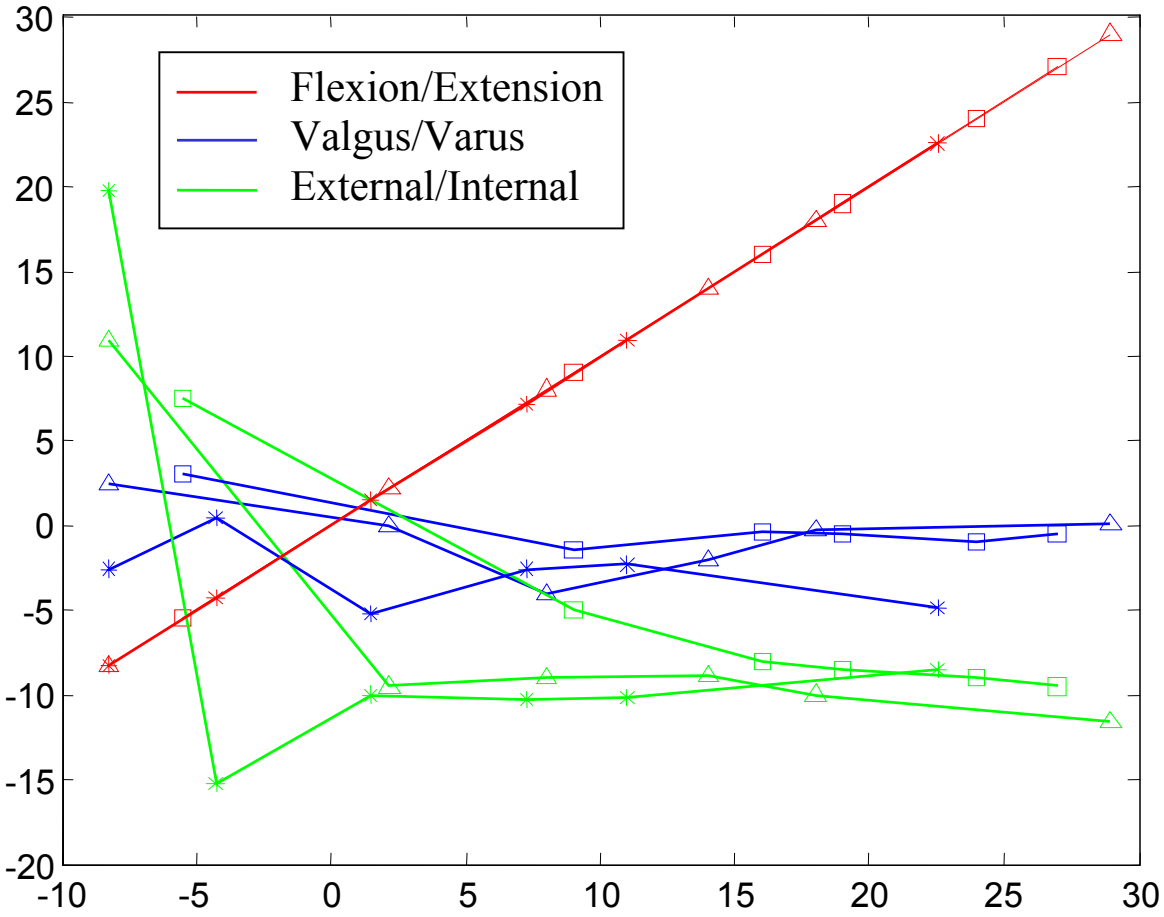

Figure 15: Three independent validation knee extension/flexion motions showing the motion of femur with respect to the tibia for Volunteer B starting from fully extended to flexed (relative to static knee flexion of 10°).

6.2.6 Registering the Cine MR Images to the Static volumes

A detailed description of the methodology and code is given Appendix A (Section 9). In brief, once the manual segments have been generated from the cine MR images and converted to binary volumes, the static binary volume for the femur is registered to the femur slices and the tibia volume to the tibial slices, using a rigid registration algorithm. This is carried out for each flexion position and an affine matrix generated for each flexion position of the femur with respect to the tibia.

6.2.7 Calculating the Euler angles

The Euler rotation angles for each flexion position are then calculated by decomposing each affine matrix in the order (Z, X, Y), where Z is the primary flexion axis, X is the valgus (+ve) / varus (-ve) axis and Y is the internal (+ve) / external (-ve) rotation axis.

7 Simulations

7.1 Mesh Template simulations

D7.3b (p11-19) described in detail the process of generating the initial template mesh and the simple rotation simulations that were carried out.

7.1.1 Simulation Issues

7.1.1.1 Penetration / Perforation Issues

One of the major reasons for the effort expended in the development of the template mesh was the difficulty encountered with the contact interfaces if initial penetrations or perforations existed. The PAM-SAFE solver requires that structures modelled as solids have an envelope of shell elements surrounding the structure created, which are then specified in the contact definition. Initial penetrations occur when the thicknesses of the shell elements overlap, whereas initial perforations occur when the centre-line to the elements intersect.

7.1.1.2 Hour-glassing

Some problems were encountered with hour-glassing of the elements forming the cartilage and meniscal solids. However, this was resolved by using the Selective Reduced Integration (SRI) option in the material definition.

7.1.1.3 Small volume elements

Although great effort has been expended in ensuring that the elements have an adequate volume (e.g. by curtailing the geometry of structures in thin regions and re-meshing), in areas such as at the edge of cartilages or to the inside edge of the menisci where it tapers, low volume elements existed, which caused problems with simulations failing early due to negative volume errors. One method that reduced these failures was to add the nodes forming small elements at the non-contacting edge of cartilages to an additional rigid body definition. This method was also helpful in reducing problems with the attached ends of the menisci.

7.1.2 Exercise rig simulations

D7.3b (7-9) discussed the development of the MR-compliant exercise rig used to load the knee during the cine MR acquisition process. Having undertaken a simple flexion rotation of the tibia about the fixed femur the next stage was to model the rig and loading conditions in PAM-GENERIS™ to flex the knee by applying a load along the long axis of the tibia.

Beams were attached to the femoral and tibial bone segments to model the appropriate lengths and masses of the limb segments, calculated from the patient measurements made by the clinician. A displacement boundary condition that prevents translations, but allows rotations for all rotational degrees of freedom was applied to the proximal node of the femur bar (to model the hip joint). The calculated force exerted by the extension of the bands of the exercise rig is applied at the distal node of the tibia bar.

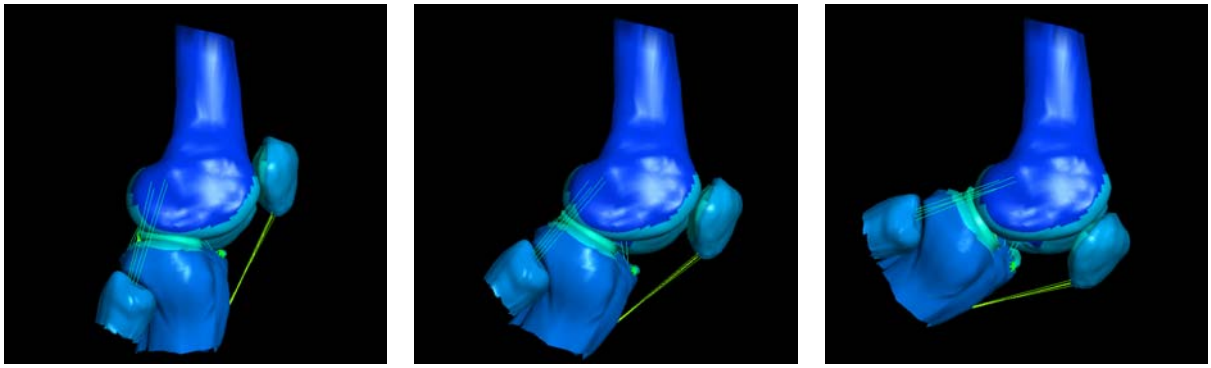

Figure 16: Initial 10° flexion

Because the static knee was imaged in a slightly flexed position (approximately 10°, as shown in Figure 16), a simulation was run to 10 degrees extension. A new flexion simulation was then run from the fully-extended position (Figure 17).

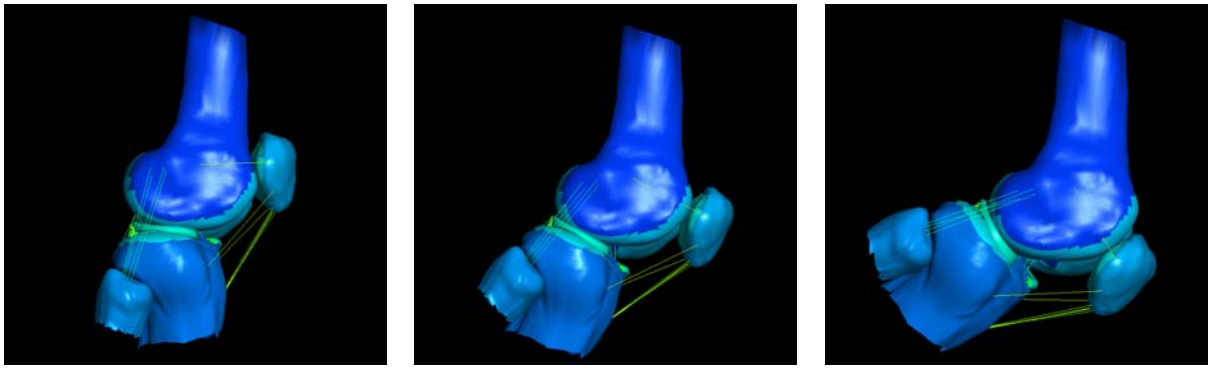

Figure 17: Fully extended knee

7.2 Patient-specific Simulations

Once the kinematic behaviour of the template knee mesh for flexion simulations had been demonstrated, it was then necessary to exercise the mesh morphing process to create patient-specific meshes and to run patient-specific simulations.

Examples of the resulting morphed meniscal meshes are shown in Figure 19, Figure 20, Figure 21, and Figure 22, while the meniscal template meshes are shown in Figure 18.

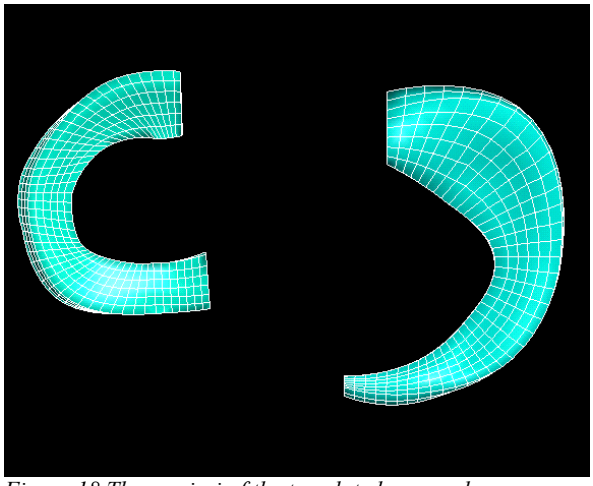

Figure 18 The menisci of the template knee mesh

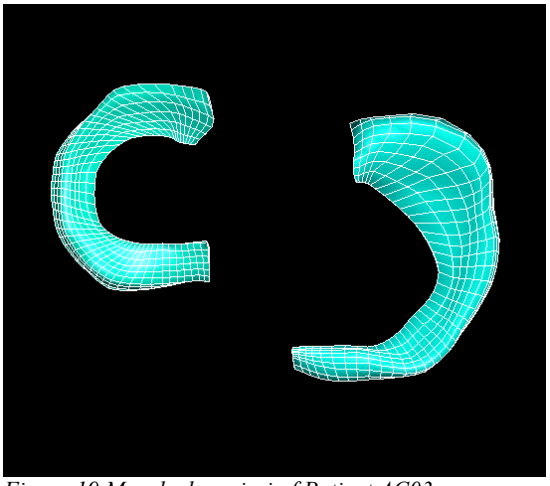

Figure 19 Morphed menisci of Patient AC03

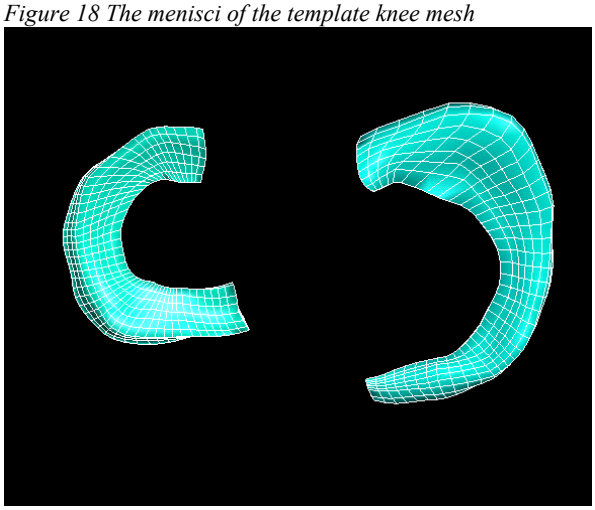

Figure 20 Morphed menisci of Patient MN02

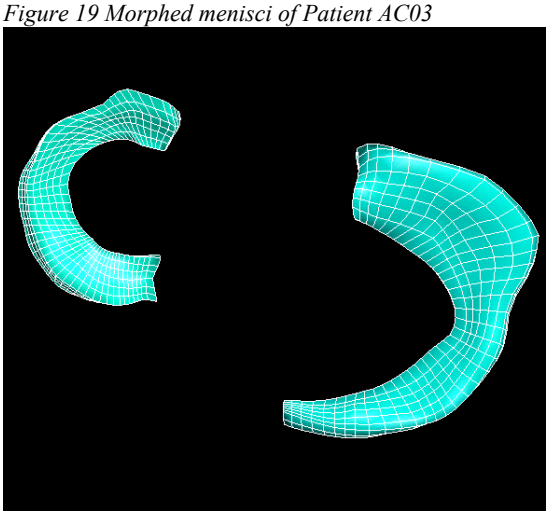

Figure 21 Morphed menisci of Patient MN03

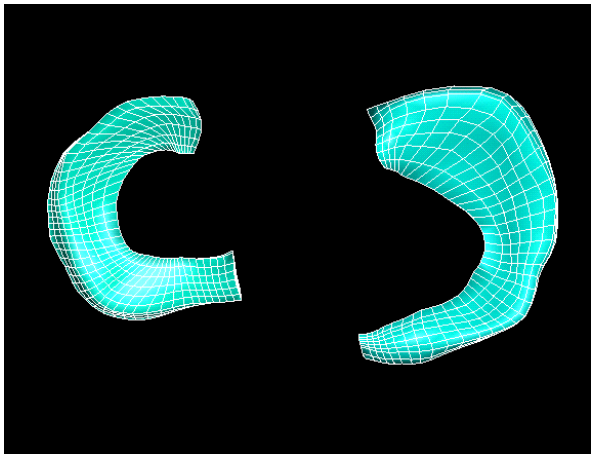

Figure 22 Morphed menisci of Patient MN07

Figures 24-27 demonstrate patient-specific femoral meshes resulting from morphing the template shown in Figure 23 The template femur mesh. In all of the meshes the condyles have remaining smooth. However, outside the region of interest, where image contrast is poor, some minor distortion of the femoral shaft has occurred, as indicated in Figure 24.

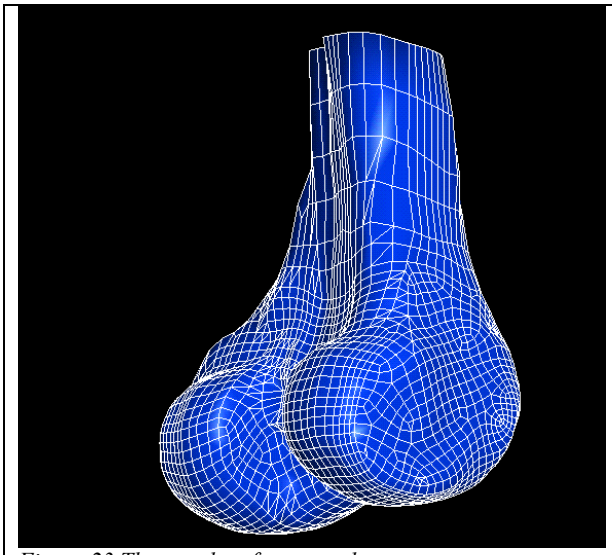

Figure 23 The template femur mesh

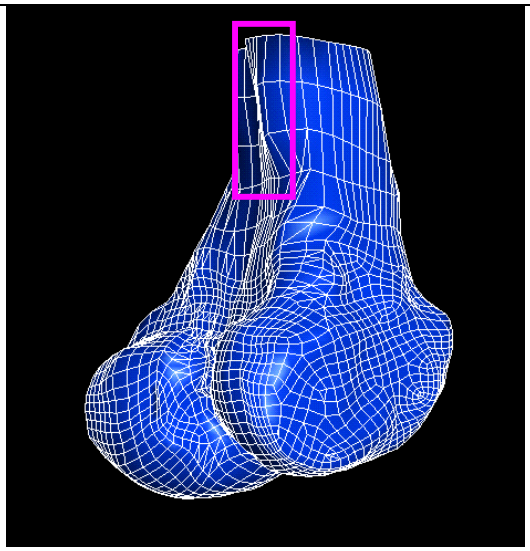

Figure 24 Morphed femur of AC03

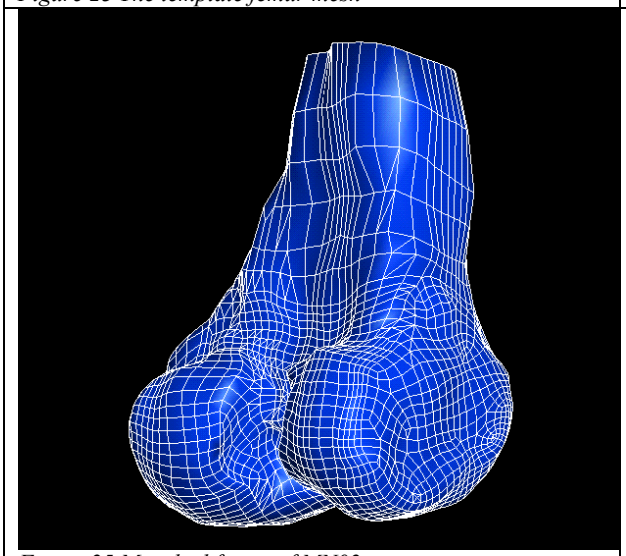

Figure 25 Morphed femur of MN02

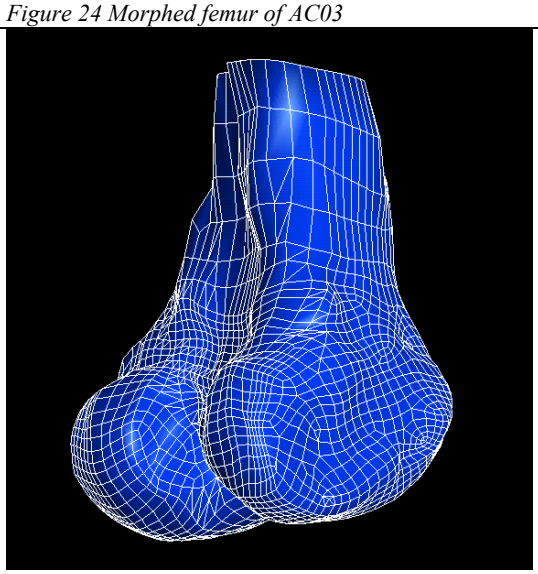

Figure 26 Morphed femur of MN03

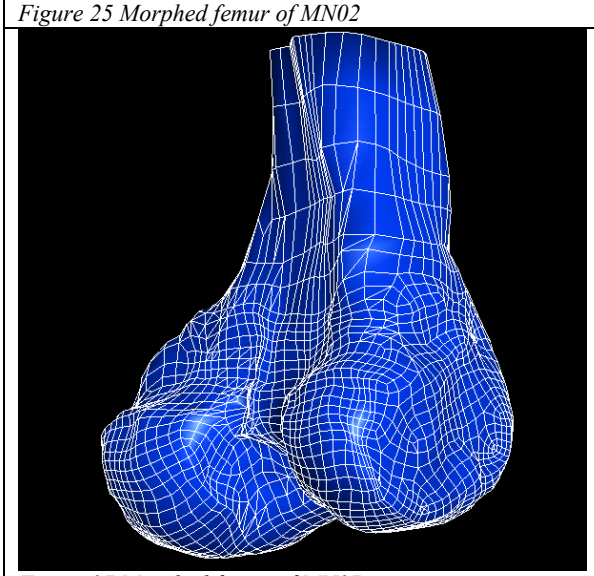

Figure 27 Morphed femur of MN07

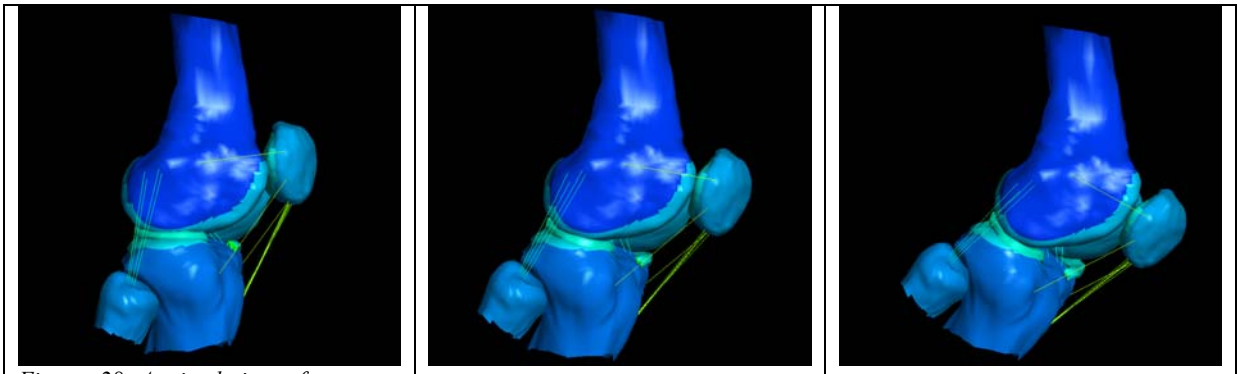

Figure 28 A simulation of postero-lateral corner injury, Patient: AC03

7.3 Validating the simulations

7.3.1 Calculating the Euler angles from the PAM simulation

To calculate the three translations and Euler angles for each simulation, a 4x4 matrix was defined for each of the femur and tibia. These matrices consisted of the nodal co-ordinates for 4 nodes on each of the femur and tibia, as shown:

$$[x]_{FEMUR} = \begin{bmatrix} x_1 & x_2 & x_3 & x_4 \\ y_1 & y_2 & y_3 & y_4 \\ z_1 & z_2 & z_3 & z_4 \\ 1 & 1 & 1 & 1 \end{bmatrix} \quad \text{and;} \quad [x]_{TIBIA} = \begin{bmatrix} x_1 & x_2 & x_3 & x_4 \\ y_1 & y_2 & y_3 & y_4 \\ z_1 & z_2 & z_3 & z_4 \\ 1 & 1 & 1 & 1 \end{bmatrix}$$

Affine matrices for both tibia and femur were calculated, as follows:

$$[A]_{TIBIA} = [x]_{TIBIA}[x_o]^{-1}_{TIBIA}$$

$$[A]_{FEMUR} = [x]_{FEMUR}[x_o]^{-1}_{FEMUR}$$

To map the tibial rotation to the femur, the following operation was performed:

$$[A_{TIBIA}]_{FEMUR} = [A]^{-1}_{FEMUR}[A]_{TIBIA}$$

This matrix takes the form of:

$$\begin{bmatrix} & [R] & & [T] \\ 0 & 0 & 0 & 1 \end{bmatrix}$$

The Euler angles for each simulation have been calculated (using the program calc_angles) from the 3x3 rotation matrix, R, and the translation vector, T.

Figure 29 indicates the rotation angles for the valgus/varus and internal/extension axes plotted against flexion for one simulation and two validation trials for the same individual (Volunteer B). Within the range of the validation motion, the simulation appears to show less axial rotation of the femur on the tibia compared with the validations. However, an external femoral rotation occurs in the same direction and with the same magnitude as the validation angles although starts from more flexed angle. Further development is necessary to investigate the reasons behind this result, but it is liable to be associated with the boundary conditions applied and the modelling of the knee ligaments.

It is likely that additional work will be required to model the complex nature of the cruciate and collateral ligaments. At the start of the programme we felt that available 3-D material models and finite elements were not developed sufficiently to address this. Current advances may permit solid modelling of the ligaments to be investigated as a post-project development. The development of a more advanced template featuring these elements is recommended. Further work is required on the measurement of muscle forces and of the pretension in ligaments to improve the applicability of the simulations to the *in vivo* condition.

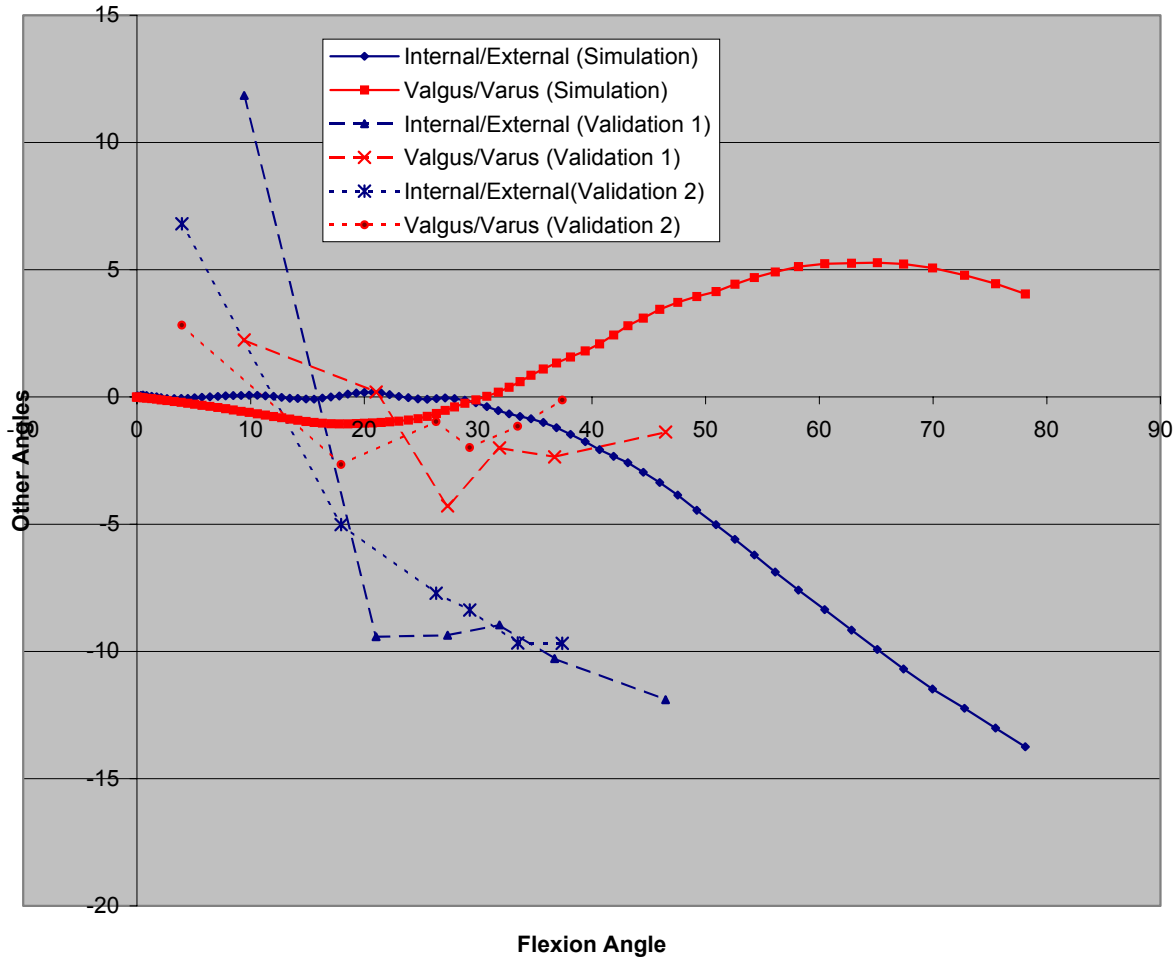

Figure 29: Validation trials (x2) for Volunteer B and the simulation rotation angles for the template mesh (Volunteer B as calculated from fully extended)

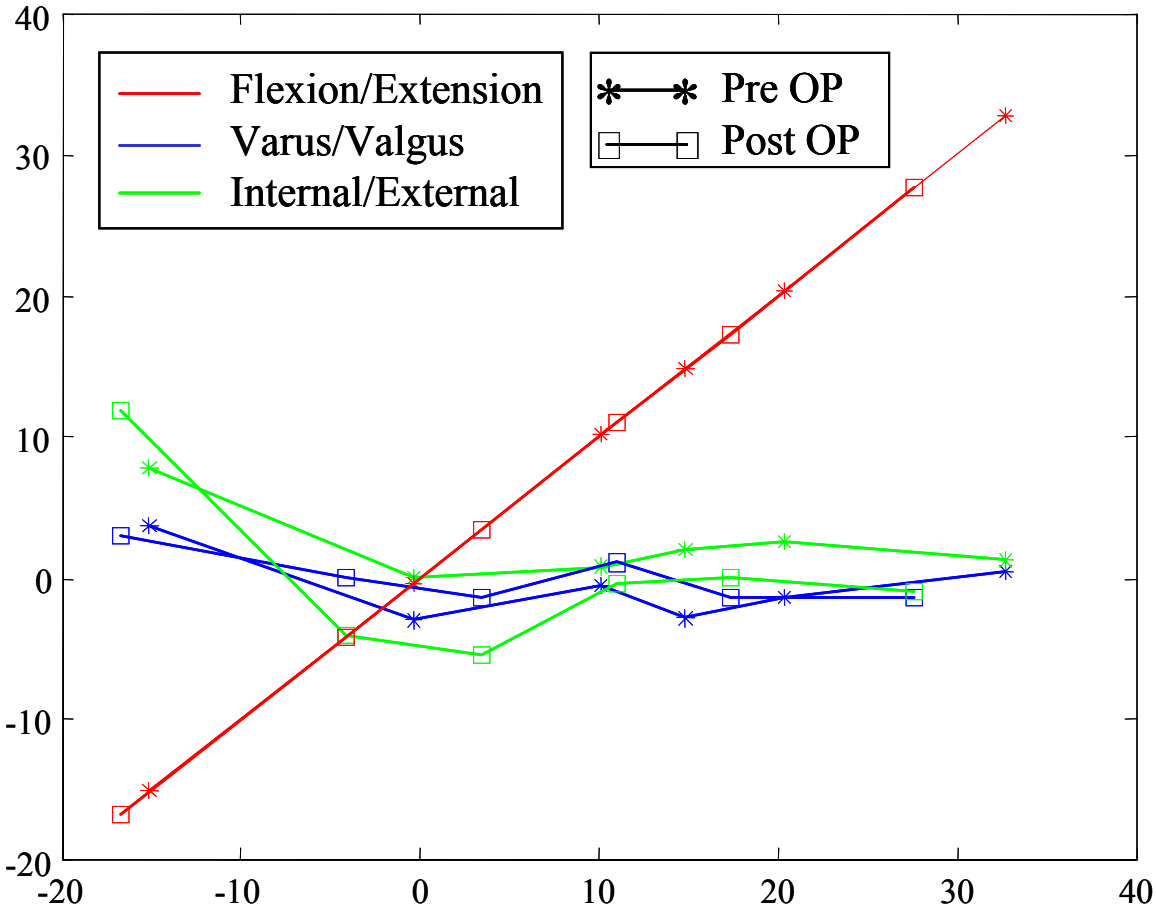

Figure 30:Pre and post-op validation plots for patient AC03 showing the rotations of the femur with respect to the tibia

The validation results for patient AC03 (the postero-lateral corner injury) are with respect to the knee flexion angle when the patient was scanned statically. Hence, the first dynamic flexion angles appear as negative angles (due to the patient having been scanned at 15° of static flexion). The pre and post-operative flexion angles indicate the difference in flexion increments for the two independent knee flexion motions. Despite the differences in increments, the internal (+ve) / external (-ve) rotations (green lines) are reasonably consistent in direction and magnitude. Both appear to indicate a "screw-home" of the femur rotating externally in the first 15° degrees knee flexion, thereafter appearing to stabilise to around neutral axial rotation. The knee appears to be relatively stable in valgus / varus (sideways tilting) with only 3-4° of range. The surgeon was not surprised by the apparent stability of the knee demonstrated from the validation results pre-operatively, because the range permitted in the MR scanner was limited and the rig itself helped to constrain the permitted motion.

Figure 31, indicates the calculated Euler angles from the pre-op simulation of patient AC03. In the flexion region of up to 45° (as indicated from the validation angles in Figure 30), the secondary rotation axes appear to be more stable than indicated from the validation results, although both the pre-op validation and the simulation results are centred around zero °. The screw-home mechanism, (indicated in Figure 30) of approximately 8° of external femoral rotation in the first 18° of knee flexion has not been captured by the simulation. In this simulation the knee had been flexed from the flexion angle used in the static MR acquisition (of 10°); thus the region in which most of the screw-home would be likely to occur had not been modelled.

Further discussions regarding the simulation and validation results, together with demonstrations of the software tools, will be made at the Final Review.

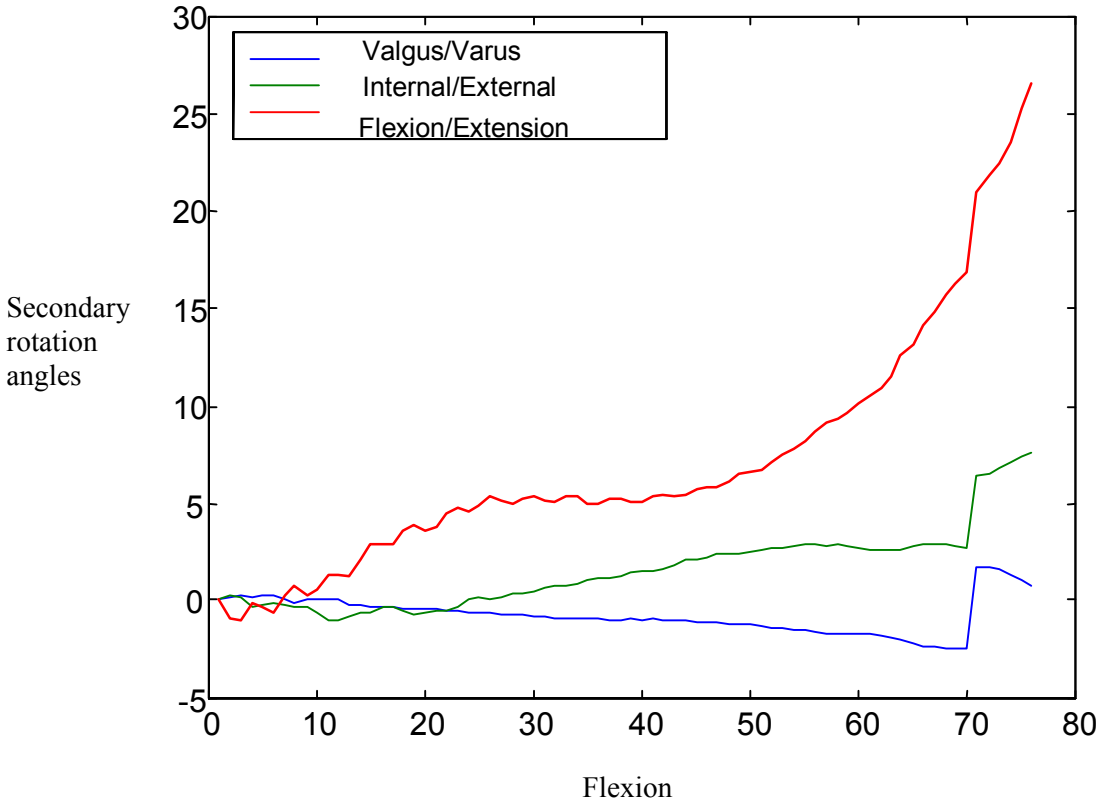

Figure 31:The calculated Euler rotation angles for the pre-op simulation of patient AC03

8 Conclusions

Although further developments for the knee simulations are required post-project, overall the Simbio Environment demonstrates a viable methodology for patient-specific simulation of knee kinematics, with potential application in surgical planning and prosthesis design. A novel automatic segmentation tool that has been developed as part of WP1 reduces the time to complete a segmentation of the bones and cartilages of a knee joint from approximately 4 days to 20 minutes, running on a high-end workstation. It is believed that the methodology would be applicable to any joint of the body. Indeed the registration algorithm developed has already been demonstrated to be applicable to the more diverse application of segmenting MUGA blood volume heart scans and renal function scans from nuclear medicine images automatically. In addition, it has been shown to work for prostate tumour segmentation from ultrasound images.

Coupled to the automatic segmentation process, is the automatic mesh generation method that has been developed for morphing an existing template knee mesh. The process is very quick once the registration process has been completed, taking less than a minute on a high-end workstation. Once again this technique is believed to be applicable to any joint in the body, and is particularly necessary for simulations that require smooth surfaces to solve articulating contact problems.

For the computationally intensive application of running kinematic simulations, the remote parallel computing aspect of the project has proved critical. Although USFD has a four processor SGI Origin 2000, which has been useful for developmental simulation work, in the clinical setting the turn around time for the simulation results would be inadequate. A typical simulation run takes approximately 7.86 hours to reach approximately 45° of knee flexion (300ms) using 4 processors of the NEC Score Cluster. In contrast, using three processors on the Origin 2000 SGI (four 250MHz R10K processors, 2560Mb RAM) at USFD the same run takes 25.8 hours. It is likely that clinicians, particularly surgeons wishing to undertake pre-operative planning, would expect a turn-around time of under 12 hours for results, including the scanning time and image processing, and thus parallel computing facilities and solvers are vital to achieving this time-scale. For hospitals that do not have access to such a computing resource, remote computing is clearly the way forward.

9 Appendix A: Dynamic Registration Process: USFD

The mechanism for deriving the rotation angles from the cine MR images has five stages.

1. The cine images must be segmented (annotated) manually. Sheffield uses the software SURFDriver to achieve this, which requires that the DICOM images are converted to bitmap format initially. The Matlab function '*dcm2bmp*' is available to achieve this. Separate sets of contours for the femur and the tibia are created. Each set includes up to a maximum of 42 contours, seven for each of the six flexion positions. SURFDriver permits a text file to be exported that consists of the X,Y,Z coordinates for each node forming a contour and for each contour that has been created.
2. The next step is to generate a Matlab-usable cell array of the contours created in SURFDriver by using the Matlab converter file '*read_surfdriver*'. A separate cell array is required for each flexion position and for each structure (i.e. the femur and the tibia).
3. Having generated the cell arrays for the contours, each is converted into a binary volume using the function '*contours2image*'. An example command to convert the first 7 contours of the tibial contour set to a binary volume is given below:
   - [tibia_vol_1] = contours2image(tibia_contours(1:7), [0.82], [419 419 7], [1 1], [ ], [1]);
4. Once the binary volumes for each of the sparse dynamic images have been generated the binary volume generated from the static MR 3-D images is registered to them using the function '*register_dynamic'*. An example command to register the first set of 7 dynamic tibial segments to the static tibia is give below:
   - [tib_out1,aff_mat_f1,dyn_full_f1] = register_dynamic(tib_vol_1,tib_vol_1mmz,dc_zlocs,[ ],[1 1 1],[1 1],[ ]);

   It is advisable to inspect the quality of the registration results visually by isosurfacing the volumes for each position and overlaying them (using a semi-transparent setting for the static volume (i.e. set(gco,'facealpha', 0.5)).
5. The final stage, once all the binary volumes have been generated, is to calculate a new affine matrix for each of the tibial flexion positions with respect to the static femur and to use the function '*calc_angles*' to calculate the rotation angles from the new affine matrix.
   - a1 = inv(aff_mat_tibia1.full_aff)*aff_mat_femur.full_aff
   - rot1 = calc_angles(a1)

   Once all of the angles have been calculated they are plotted in Matlab.

USFD/STHT Matlab Dynamic Registration Functions

dcm2bmp

dcm2bmp converts MRI dicom files into bmp files.
Usage: dcm2bmp(infile, outfile, number of slices,intensity value, left or right knee)
dcm2bmp uses the USFD dcmread function
Before converting a batch, test the intensity scaling using just 1 image

read_surfdriver

contour = read_surfdriver('file.txt')
Where, contour = suitable name for the cell array and file.txt is the contours file exported from surfdriver in ascii format.

contours2image

[new_vol]=contours2image(in ,resol_in, vol_size, vox_size, vol, tag);

This function will build and render the volumes from the cell array of curves generated by matlab's 'read_surfdriver' function.
(read_surfdriver requires a contour text file exported from surfdriver)

in – the Matlab cell array containing the contours e.g. tibia_contours
resol_in – the in-plane pixel resolution of the image from which the contours were built e.g. [0.82]
vol_size - the number of pixels in each direction for the volume produced e.g. [419 419 7]
vox_size - the dimensions in mm of the voxels for the output volume e.g. [1 1]
vol - an already existing empty volume for the contours to be added to e.g. [ ]
tag - the number to fill the volume with e.g. [1]

new_vol - the binary volume data set e.g. [tibia_vol_1]

register_dynamic

[out, ctf_out, dyn_full]=register_dynamic(dynamic, static, dynam_z,roi, vdim_static, vdim_dynam, guess)

Where :
dynamic - The dynamic data set for registration, typically 7 slices
static - The initial high quality static volume data set.
dynam_z - A 1xN vector containing the depth location of each slice in the dynamic data set. This is derived typically from Efilm.
roi - A data array the same size as dynamic with zeros and ones indicating the regions to be used in the registration. Default +/- 10% of the image dimensions.
vdim_static - An 1x3 vector containing the [x y z] dimensions of each voxel in the static data set. Default is [1 1 1]
vdim_dynam - A 1x2 vector containing the [x y] dimensions of each voxel in the dynamic data set. Default [0.82 0.82] (which assumes the USFD 419 x 419 FOV and 512 x 512 matrix)
guess - A best guess of the likely transformation, in the case of dynamic knee flexion it would be the affine matrix from the previous flexion angle.

The final 2 options need not be specified and the defaults will be used

calc_angles

angle1 = calc_angles(a1)
*Where a1 = the inverse of the full affine of the tibia * the full affine of the femur*
*a1 = inv (aff_mat_tibia.full_aff) * aff_mat_femur.full_aff*